Geochemical Journal, Vol. 47, pp. 137 to 147, 2013

Tectonics and mechanism of a spreading ridge subduction at the Chile Triple Junction based on new marine geophysical data

TAKESHI MATSUMOTO,[1]* ASUKA MORI,[2] SHINICHIRO KISE[1] and NATSUE ABE[3]

[1]University of the Ryukyus, 1 Senbaru, Nishihara-cho, Okinawa 903-0213, Japan
[2]Global Ocean Development Inc., 1-13-8, Kamiooka-Nishi, Konan-ku, Yokohama 233-0002, Japan
[3]Japan Agency for Marine-Earth Science and Technology, 2-15 Natsushima-cho, Yokosuka 237-0061, Japan

(*Received February 22, 2012; Accepted March 22, 2013*)

The Chile Triple Junction (CTJ), an RTT-type triple junction located at 46°13′ S, 75°48′ W off the western coast of Chile, is characterized by the subducting Chile Ridge, which is the constructive plate boundary that generates both the Nazca Plate and the Antarctic Plate. The ridge subduction mechanism and the regional tectonics around the CTJ were investigated primarily using marine geophysical data (topography, gravity, geomagnetic field and single-channel seismics) collected during the SORA2009 cruise (Cruise ID = MR08-06) by R/V MIRAI together with other cruise data from the National Geophysical Data Center. The segment of the ridge axis just before the subduction around the CTJ is associated with an axial deep covered with thick sediment unlike that seen in typical ridge crests. The profiles of both topography and the free air anomaly around the CTJ show quite different patterns from those of ordinary subduction zones. However, topographic features typical of a slow-spreading type ridge, including a median valley and both flanks, remain in the seaward side of the trench. Even after the subduction of the eastern flank, the topographic features of the western flank remain. A slight Outer Rise and an Outer Gravity High, which are common in the western Pacific area, were observed in an area far away from the CTJ on both Nazca and Antarctic plate sides. The geomagnetic anomaly pattern around the Chile Ridge near the CTJ shows that the estimated spreading rate decreases gradually towards the ridge crest. This suggests that volcanic activity diminishes gradually towards the subducting ridge axis. The lithosphere under the Chile Ridge might have amalgamated with the surrounding oceanic lithosphere due to heat loss after the cessation of volcanic activity. The oceanic lithosphere towards the trench also thickens rapidly due to heat loss. Consequently, shallow-angle subduction of the youngest and most immature oceanic plate occurs smoothly via slab-pull force without any resistance along the interface between the South American continental plates.

Keywords: Chile Ridge, Chile Triple Junction, Chile Trench, Outer Gravity High, slab-pull

INTRODUCTION

The Chile Triple Junction (CTJ), an RTT-type triple junction located off Taitao Peninsula on the western coast of Chile, is remarkable in that the Chile Ridge is subducting obliquely underneath the South American continental plate (Fig. 1). The CTJ is therefore the junction between the Nazca, Antarctic, and South American plates (Lagabrielle *et al*., 2000). The Nazca Plate, north of CTJ, is converging with the South American Plate at 7–8.5 cm/yr. towards ENE, whereas the Antarctic Plate is converging at 2 cm/yr. towards the east where the ridge has already been subducted (D'Orazio *et al*., 2000; Veloso *et al*., 2009). The water depth at the Peru–Chile Trench axis, located west off the coast of the South American Continent between 40°S and 50°S, is 3,000–4,000 m. The meandering Mornington submarine channel, a possible passage for large amounts of terrigenous sediment, is located on the continental slope off the coast of the South American continent near the CTJ. The Chile Ridge is split into segments by transform faults with spacing of 50–250 km (Fig. 1).

The CTJ has been studied by various disciplines. The area north of 46°S is a seismically active zone whereas the area around 46°30′ S is seismically inactive (Tilmann *et al*., 2008). A gap to the volcanic front on land is located at 46°30′ S (Stern, 2004). The study area is also characterized by 5.6–5.2 Ma ophiolite exposure on the Taitao Peninsula at 46°40′ S, 75°30′ W (Anma *et al*., 2006).

A re-construction model of the Pacific basin based on the paleo-magnetic frame (Smith, 2003) shows that most areas of the Pacific Rim have already been affected by similar ridge subduction. For example, the Pacific–Izanagi ridge was subducted under the Japan Trench during the Cretaceous period (Smith, 2003). The Pacific–Phoenix ridge was subducted under the Antarctic Plate in the Early

*Corresponding author (e-mail: tak@sci.u-ryukyu.ac.jp)

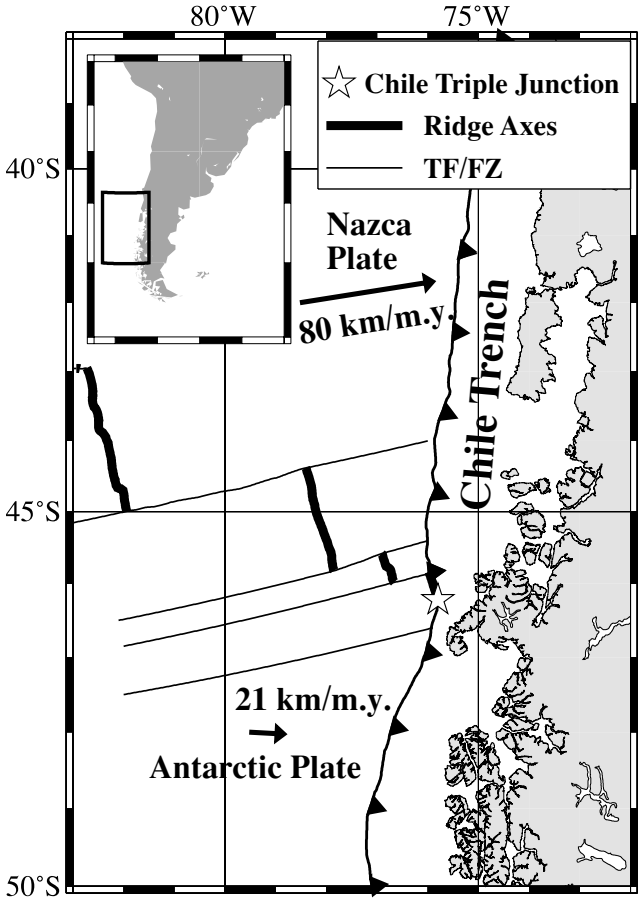

Fig. 1. Tectonic map of the study area off the Chilean coast. The T-T-R type Chile Triple Junction (CTJ) located off Taitao Peninsula (the star located around 46.2°S, 76.8°W on this map) is the junction of the Nazca, Antarctic, and South American Plates. The Nazca Plate is subducting underneath the South American Plate towards N81°E at a rate of 80 km/m.y. (8.0 cm/y) whereas the Antarctic Plate is subducting towards N93°E at a rate of 21 km/m.y. (2.1 cm/y) around the CTJ, both based on the NUVEL-1A plate model (DeMets et al., 1994). Bold lines show axes of the Chile Ridge segments and thin lines show active transform faults and fracture zones ("TF/FZ" on the legend.)

Tertiary. However, no relics of ridge subduction were identified on the landward side of the trench around the Pacific Plate. Spreading ridges are characterized by presence of ridge-axis discontinuities due to heterogeneous upwelling of magma (Macdonald *et al*., 1988). It might be difficult for a spreading ridge to subduct smoothly underneath a trench because the ridge is supported by the buoyancy of young, hot crust and is in isostatic equilibrium. The subduction of a spreading ridge may be delayed compared with that of neighboring flat sea floor and as a result, it may form a cusp in the trench axis.

The purpose of this study is to provide an explanation for the mechanism of smooth subduction of the spreading ridge into the trench through regional tectonics around the CTJ, mainly based on the marine geophysical data collected by the recent R/V MIRAI SORA2009 cruise (Abe, 2009) together with other cruise data from the National Geophysical Data Centre.

Data and Results

SORA2009 cruise data

An overall geophysical and geological study of the area, including the southern East Pacific Rise and the CTJ, was carried out during the SORA2009 Cruise by R/V Mirai (Cruise ID: MR08-06 Leg1b) from 6th February until 14th March 2009. Precise sounding and topographic mapping was conducted using a SEABEAM 2112.004 swath bathymetric survey system. Gravity measurements were conducted using a LaCoste & Romberg S-116 Air-Sea Gravity Meter. Figures 2 and 3 show the track lines across the Chile Ridge and the Chile Trench during the cruise. Figures 4(a)–(e) show selected profiles from the geophysical surveys. The 2-D Bouguer anomaly is calculated assuming a crust density of 2,670 kg/m^3 and a sea water density of 1,030 kg/m^3 based on the free air anomaly and the topographic profile projected onto the transect perpendicular to the trench axis. The MR-Line1 crosses the ridge crest 50 km west of the trench axis. The topographic profile of the western side of the ridge shows typical Mid-Atlantic Ridge-type features with a V-shaped axial valley and rough topographic reliefs on the flank. On the eastern side, this feature disappears abruptly, having a flat bottom near the trench axis. The free air anomaly reaches a minimum at the trench axis then becomes relatively negative nearby exhibiting a good correlation with the topography on the landward side and a poor correlation to the seaward side of the trench. The MR-Line2 transits along the fracture zone, therefore only a slight V-shaped axial valley is observed along the track. The MR-Line5 is located south of the CTJ. Therefore, the crustal age becomes older towards west. The water depth tends to be shallower towards the east (trench-wards).

A single-channel seismic (SCS) survey was also carried out along and across the Chile Ridge off the Taitao Peninsula. The equipment's specifications are summarized as follows:

(1) The active section length, hydrophone interval, lead-in cable length, and receiver depth of the streamer are 65 m, 1 m, 135 m, 5.2–7.8 m, respectively, and,

(2) The volume, air pressure, source depth, and dominant frequency (–6 dB) of the source are 150 in^3 (G45, I105) or 210 in^3 (G105, I105), 2000 psi, 5.2–8.0 m, and 10–85 Hz, respectively.

Six SCS survey profiles were obtained from off the Taitao Peninsula during the SORA2009 cruise. The pro-

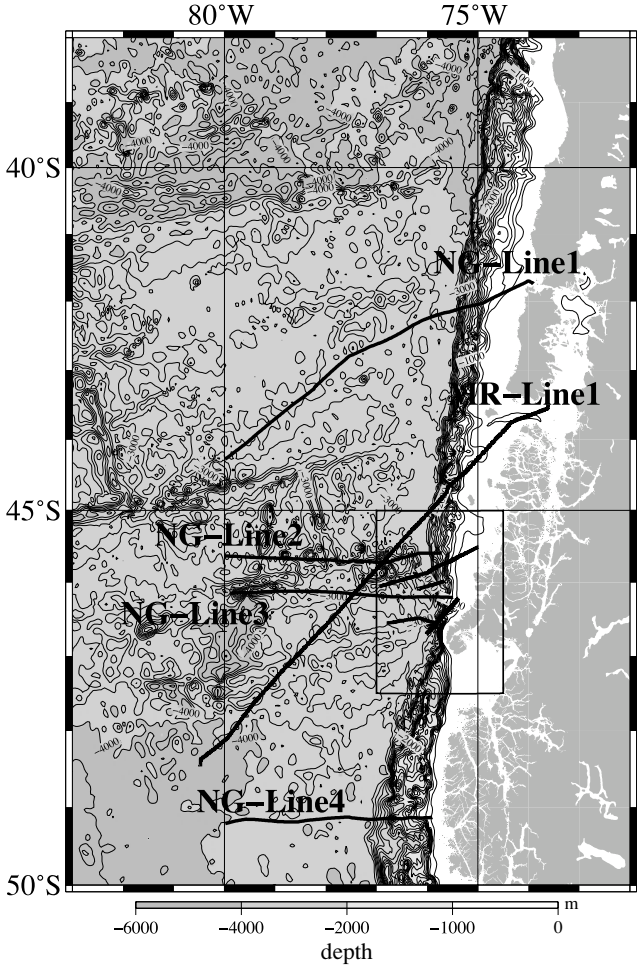

Fig. 2. All the track lines that are used in this study for topography and gravity profiles across the Chile Trench with the topographic contours based on the NOAA/NGDC ETOPO1 1-minute-of-arc grid data. The profile numbers prefixed by "MR-" are from the SORA2009 cruise by R/V MIRAI and those by "NG-" are from the geophysical data downloaded from NOAA/NGDC Marine Trackline database. Details of the short tracks around Taitao Peninsula are shown in Fig. 3, the area of which corresponds to the box on this map.

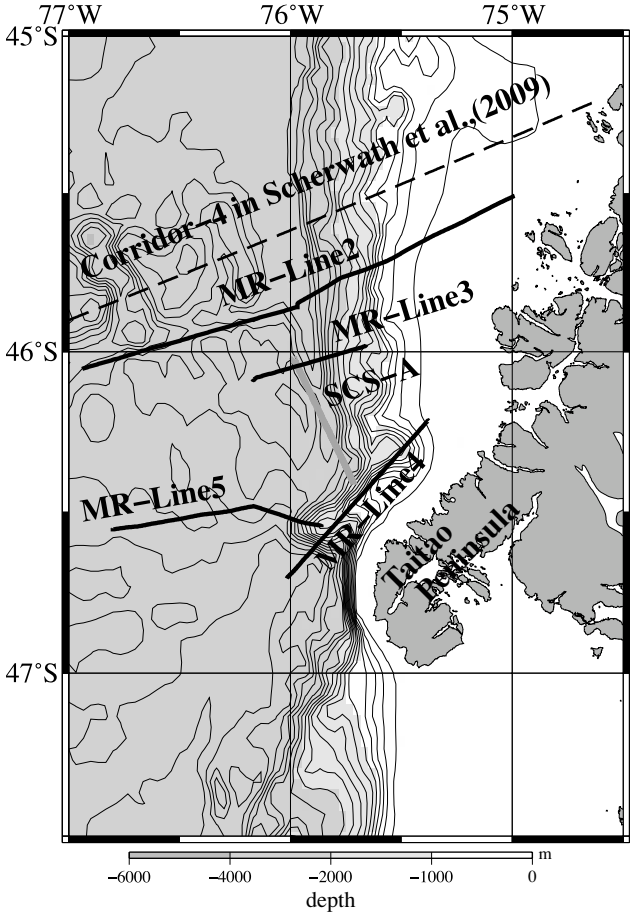

Fig. 3. Short tracks for the geophysical surveys around the Taitao Peninsula. The grey line "SCS-A" is the track surveyed by single channel seismic profiling during the SORA2009 cruise. The location of the track of Corridor 4 in Scherwath et al. (2009) is also shown in this figure.

file used in this article (SCS-A in Fig. 3) was taken along the Chile Ridge crest. Figure 3 also shows the seismic survey track (Corridor-4) that is used in this discussion. Figure 5 shows the result of the seismic reflection profile together with the interpretation of the sub-seafloor structures.

Three-component geomagnetic data were obtained by a FRG Fluxgate type shipboard magnetometer (Tierra Tecnica Inc.) 16 times per second. The raw data are processed using the synchronously obtained pitch, roll, and heading data to obtain earth-referenced X (positive northwards), Y (positive eastwards), and Z (positive downwards) components (Isezaki, 1986).

NGDC marine trackline gravity data

Since the number of the long transects across the Peru–Chile Trench and Chile Ridge is very small, and the survey area was limited during the SORA2009 cruise, geophysical (topography and gravity) data archived by NGDC/NOAA (National Geophysical Data Center/National Ocean and Atmosphere Agency) were used to complement the SORA2009 geophysical data. Long gravity transect profiles from far north (on the Nazca Plate) and far south (on the Antarctic Plate) across the ridge and the trench are mainly used in this study. Locations of the tracks are shown in Fig. 2. Data used are from the following five cruises: ELT28 (Eltanin, 1967), RC1802 (Conrad, 1975), RC1803 (Conrad, 1975), RC2107 (Conrad, 1978), and RC2304 (Conrad, 1982). Figures 6(a)–(d) show the selected topography and gravity profiles from these data. The Bouguer anomaly was also calculated by the same procedure as used in the case of the

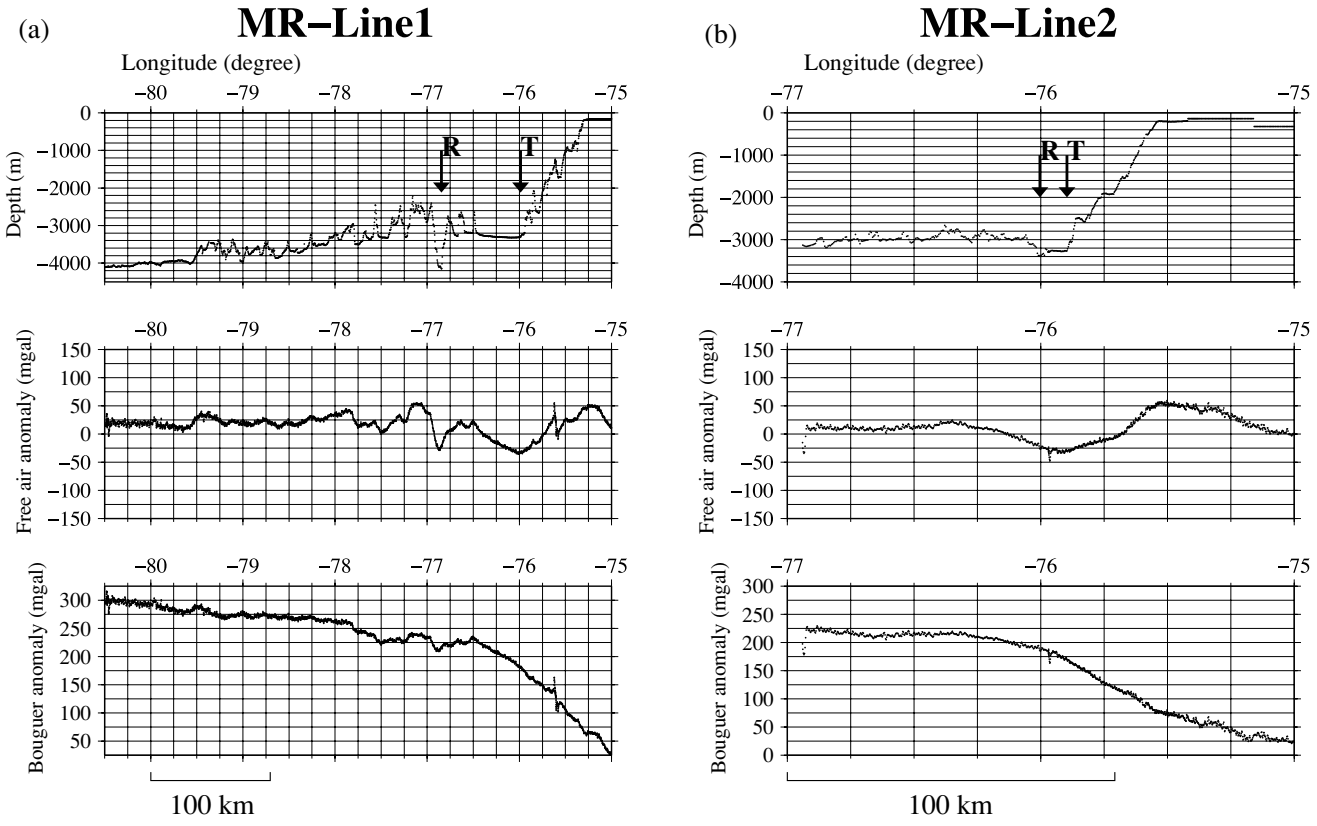

Fig. 4. Topography, free air anomaly and Bouguer anomaly profiles along the selected across-trench tracks during the SORA2009 cruise. (a) Track MR-Line1, (b) Track MR-Line2, (c) Track MR-Line3, (d) Track MR-Line4, (e) Track MR-Line5. "R" and "T" correspond to the location of the Chile Ridge crest and the Chile Ridge axis, respectively.

SORA2009 data. A slight Outer Rise and Outer Gravity High (details of these terms are explained in the discussion section) were observed along NG-Line1, which is far north of the CTJ. However, no Outer Rise or Outer Gravity High was observed in the subducting Antarctic Plate far south of the CTJ (NG-Line4). These profiles show quite different patterns in topography and gravity from other western Pacific margins (Japan Trench, Isu–Bonin–Mariana Trench, Philippine Trench, etc.). The NG-Line3 corresponds to the CTJ and shows that the V-shaped ridge crest is still preserved at the contact point to the trench axis.

Discussion

Seafloor features and gravity anomalies on the seaward side of the Chile trench

Generally, the seaward side of the trench is characterized by a topographic high parallel to the trench axis, called the "Outer Rise" or "Outer Swell". The Outer Rise usually accompanies a local high of the free air anomaly (referred to as "Outer Gravity High" hereafter), by about several tens of mgals (Watts and Talwani, 1974). Both of these topographic and gravity features are interpreted as the effect of the upward elastic bending of the oceanic plate just before subduction. However, Outer Gravity High is usually observed even without a recognizable Outer Rise, and can be interpreted as the result of abrupt thickening of the lithosphere due to heat loss before subduction at the trench axis (Tomoda *et al.*, 1983). These topography and gravity features are common along the western Pacific plate convergent margins. Scherwath *et al.* (2009) reported topographic and gravity profiles across the Chile Trench between 43°S and 46°S, north of the CTJ. They found that both the high-frequency topography and gravity features of the Chile Ridge's eastern flank are obliterated by the trench-ward subsidence in the profiles near the CTJ.

The Profile NG-Line1 located in the Nazca Plate far north from the CTJ is characterized by a typical "Outer Rise" and "Outer Gravity High" on the seaward side of the Chile trench, as shown in Fig. 6(a) (Stage-1). As the Chile Ridge segment approaches the trench, the eastern ridge flank starts subducting, as shown in Figs. 4(b), 4(c) and 6(b) (Stage-2). During this stage, the topographic features at the ridge crest (a median valley) and in both

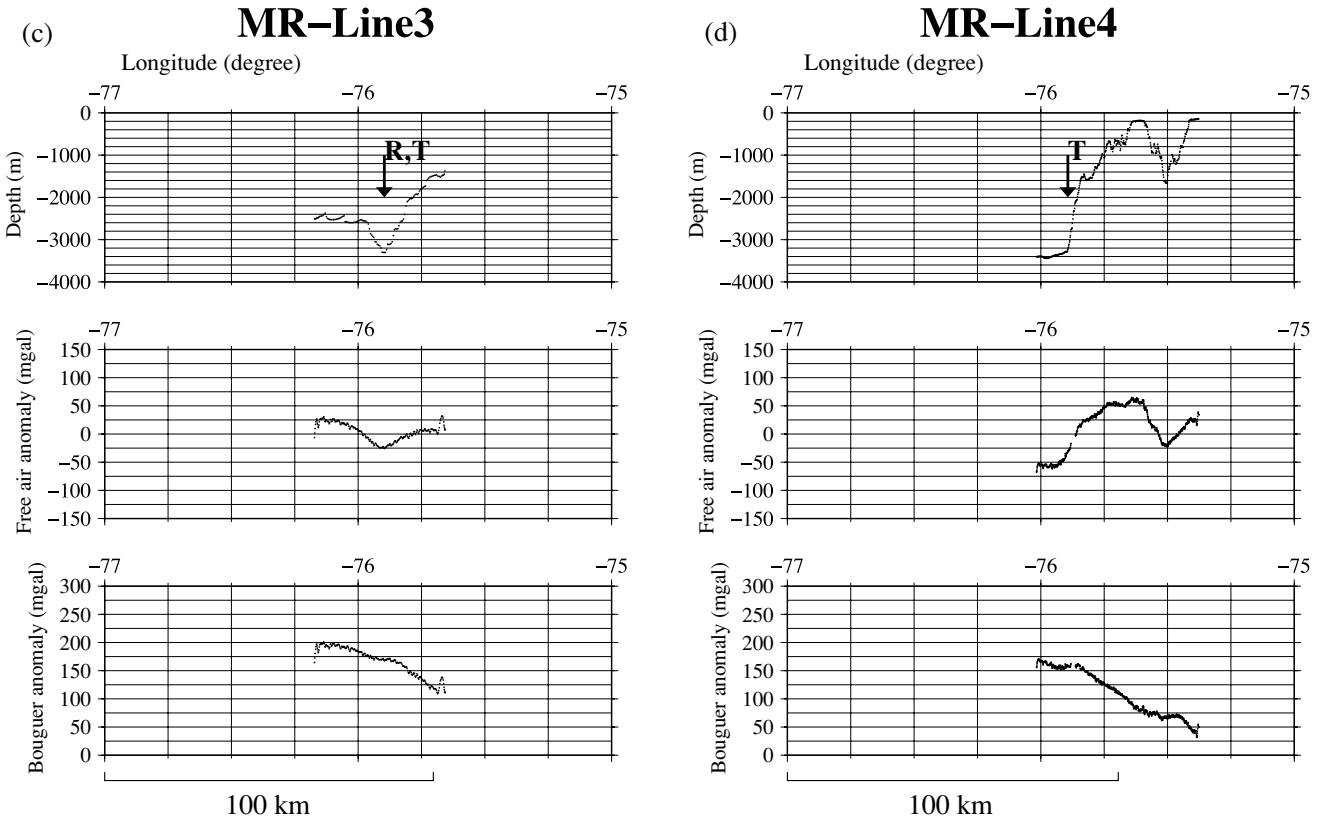

Fig. 4. (continued).

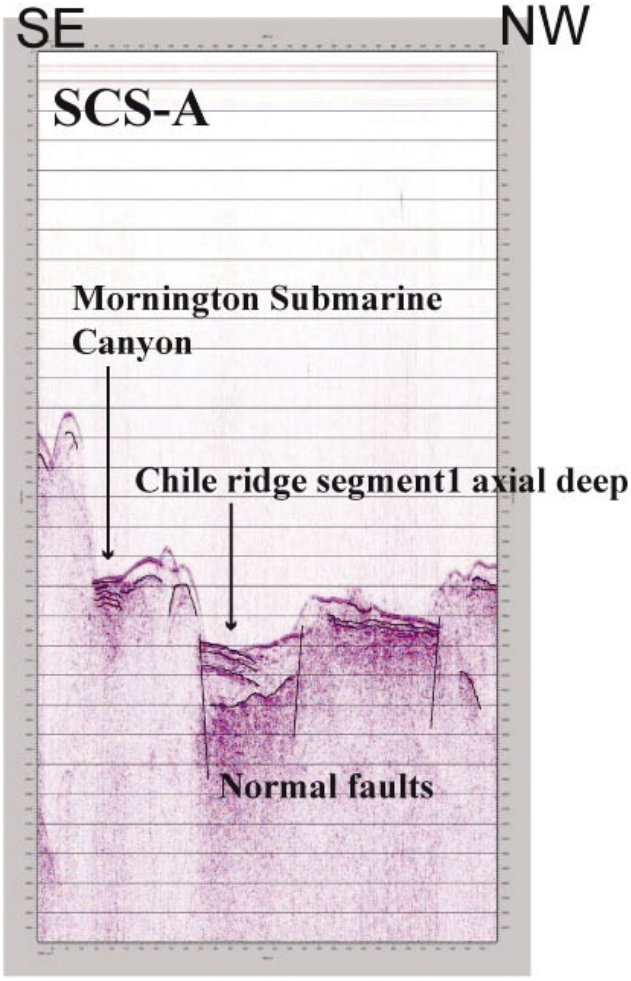

Fig. 5. Reflection profiles of the SCS survey track with the interpretation of the basement-sediment structure. The track is from the spur off the Taitao Peninsula (SE) across the Mornington Submarine Canyon, then along the V-shaped ridge crest of the segment nearest to CTJ. The observation of the acoustic basement along the ridge crest shows that the sediment thickness is not constant along the ridge.

flanks remain recognizable. Then, the entire eastern flank subducts, and only the axial valley and western flank of the ridge remain near the trench axis, as shown in Fig. 6(c) (Stage-3). Finally, the western flank of the ridge completely subducts. To the south of the CTJ, the Outer Rise appears again in the Antarctic Plate, as shown in Fig. 6(d) (Stage-4).

It is noteworthy that the same pattern appears in the topography and gravity both distantly north and south of the CTJ, although younging direction of the oceanic crusts is opposite between Stage-1 and Stage-4. In the former case, the age increases towards the trench because the spreading Chile Ridge is located to the west. In contrast, the age of the Antarctic Plate becomes younger towards the east because the ridge already subducted underneath the South American Plate.

During Stages-2 and -3, a topographic high appears in the seaward side of the trench. However, this is different from the outer rise, which is due to the elastic bending of the oceanic plate just before subduction. This topographic high is due to the topography of the ridge flanks. A relatively negative Bouguer anomaly of some 20–30 mgals is observed around the median valley before subduction (Figs. 4(a), 4(c) and 6(b)), which might be due to a buoyant crust underneath the ridge crest as described in the crustal structure by Scherwath *et al*. (2009). However, the gravity pattern disappears when the eastern flank has been subducted completely (Fig. 6(c)).

Sediment structure at the Chile Ridge crest

The topographic features of the Chile Ridge crest with the median valley (Figs. 1, 4(a), 4(c), 6(b) and 6(c)) suggest that the ridge can be categorized as the Mid-Atlantic Ridge type (Hill, 1959). Unlike the normal spreading ridge, the median valley of the active-spreading Chile Ridge near the trench, however, is characterized by a thick sediment cover on the basement rock in the SCS structure (Fig. 5). The unusually thick sediment on the ridge crest could be attributed to two factors: a sizeable amount of terrigenous sediment supplied from the Chilean continent and/or a weakening of magmatic activity along the ridge crest as the ridge approaches the trench axis.

Geomagnetic anomaly relevant to the spreading rate around the CTJ

Based on the spreading rate analysis of the magnetic profiles perpendicular to the Chile Ridge segments between 37°S and 46°S, Tebbens *et al*. (1997) suggested that the average half-spreading rate on both sides of the ridge axis decreased with time during the past 25 million years, 6.1 cm/year before 18 Ma, and 3.1 cm/year after 6 Ma. This paper also asserts a correlation between the time intervals of decreases in the spreading rate and the collision of a segment of the Chile Ridge against the Chile Trench. If this is the case, the ridge-trench collision and subsequent decline of magmatic activity at the ridge segment affected the spreading rate of the whole ridge system. To elucidate such processes, a high precision analysis of the spreading rate variability at the site of the ridge-trench collision is essential.

However, the study area especially around the CTJ has very few geophysical transects even in the NGDC Marine Trackline catalogue. Therefore, the current Mirai cruise data are of great importance to complement the poor coverage by geophysical survey tracks in this area and to interpret the CTJ tectonics. The transect of MR-Line1 in Fig. 2 crosses a couple of ridge segments. The

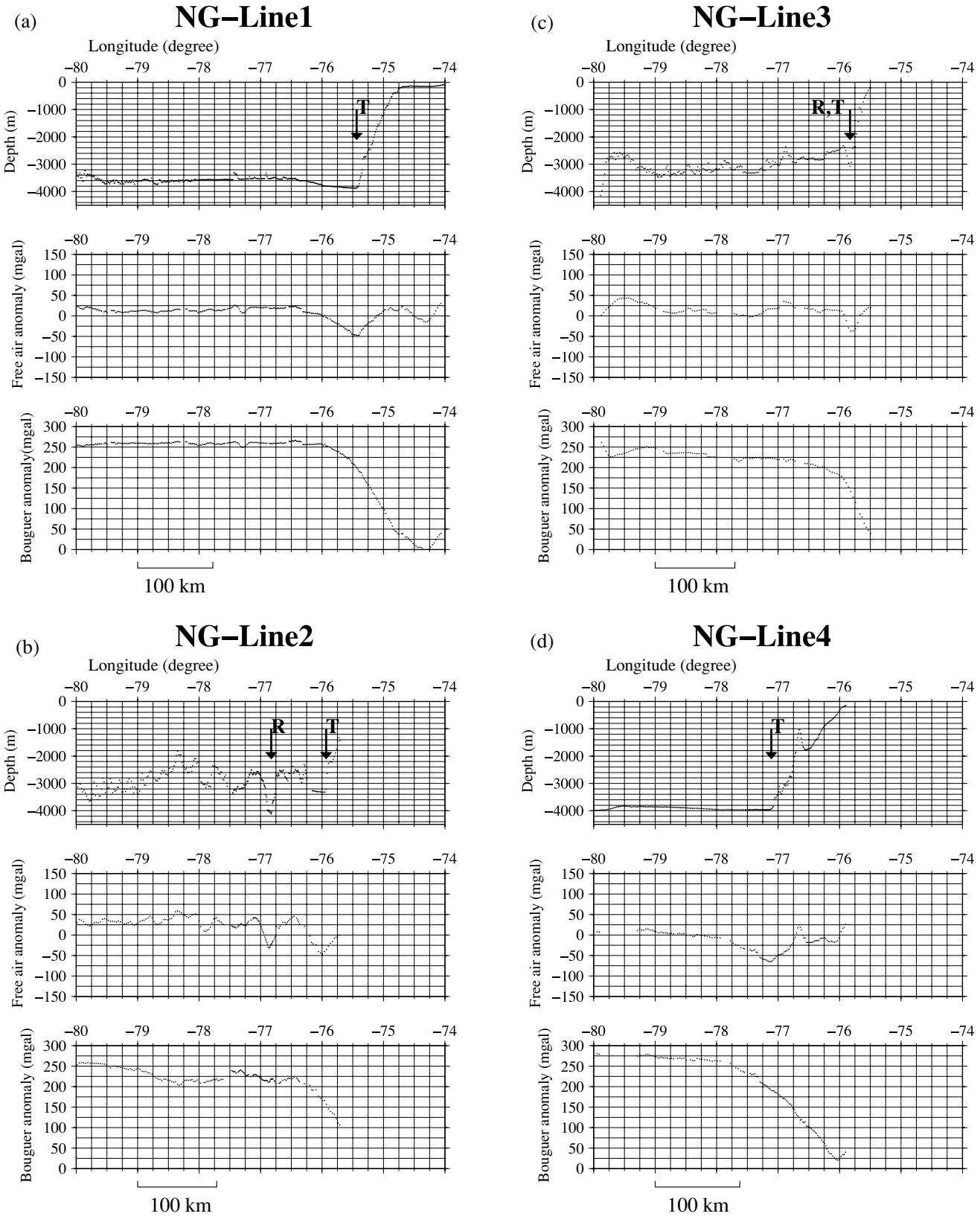

Fig. 6. Topography, free air anomaly and Bouguer anomaly profiles along the selected across-trench tracks from the NOAA/ NGDC Marine Trackline data. (a) Track NG-Line1, (b) Track NG-Line2, (c) Track NG-Line3, (d) Track NG-Line4. "R" and "T" correspond to the location of the Chile Ridge crest and the Chile Ridge axis, respectively.

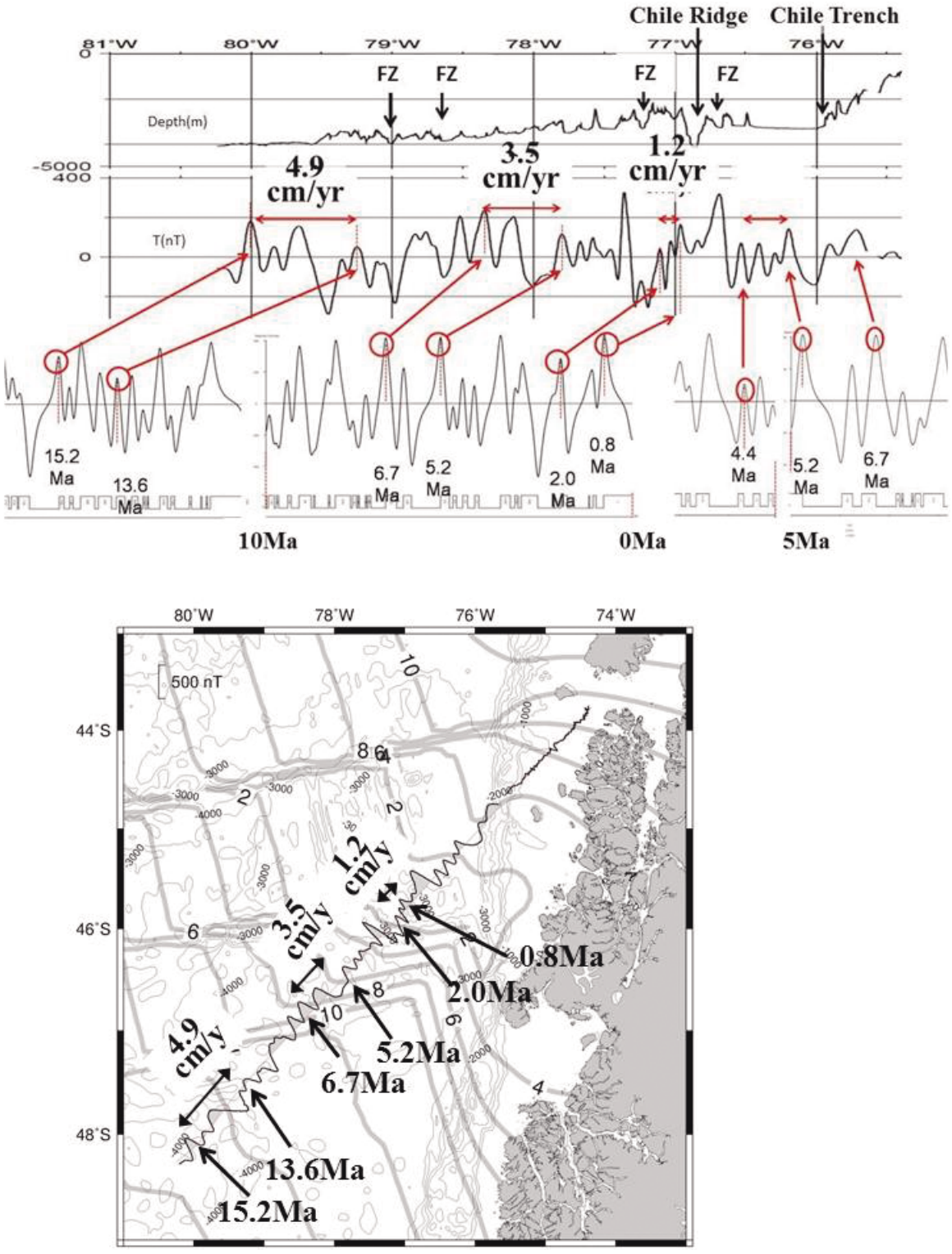

Fig. 7. The result of the estimation of the seafloor age and spreading rate based on the geomagnetic data along Track MR-Line1 (see Fig. 3). (Top) Topography, total force anomaly calculated from the three component data, and the result of the age model fitting. (Bottom) Total force anomaly profile along the track with the seafloor age estimated in this study. Grey bold lines are contours of the isochron model by Müller et al. (2008).

seafloor age around the CTJ was estimated from the total force anomaly calculated using three component magnetic data. Figure 7 shows the results of the age model fitted with the estimated half-spreading rate, and the total geomagnetic force anomaly along the MR-Line1 superimposed on the isochrons based on the seafloor age model suggested by Müller *et al*. (2008).

The spreading rate in this transect tends to decrease gradually towards the ridge axis around the CTJ, as shown in Fig. 7. The half-spreading rate gradually decreases towards the east, 4.9 cm/year around 14 Ma, 3.5 cm/year around 6 Ma, and 1.2 cm/year around 0.8 Ma in the western side of the Chile Ridge crest. This might suggest that magmatic activity along the ridge decreases gradually as the ridge crest approaches the trench and ceases completely at the trench axis due to the heat loss. This will be also discussed from the viewpoint of the lithospheric thickness in the next section.

Thickness anomaly of the oceanic lithosphere before subduction

One indicator of the thickness variability of the oceanic lithosphere is RGA (Residual Gravity Anomaly), proposed by Yoshii (1972, 1973). RGA is defined as:

$$RGA = FA - 2\pi k^2 \sum H_i(\rho_i - \rho_m)$$

where FA, k^2, and ρ_m indicate the free air anomaly, gravitational constant and uppermost mantle (lid) density, respectively. H_i is the thickness of the i-th layer of the crust obtained by seismic refraction/reflection studies. The density of the i-th layer of the crust, ρ_i, is converted from its seismic velocity based on the assumption of Nafe and Drake's (1957) empirical law. RGA, thus, is the gravity anomaly with respect to a case where the densities of the entire crustal layer and seawater are replaced by the density of the uppermost mantle (lid). Given that the most prominent discontinuity below the Moho surface is the interface between the lithosphere and asthenosphere, RGA can be used as a proxy of lithospheric thickness. If no heat generation within the lithosphere is assumed in the 1-D thermal equation, lithospheric thickness, and hence the relative increment of RGA, are proportional to the square root of the age (Yoshii, 1973). A 100 mgal difference in the RGA corresponds to a 24 km difference in lithospheric thickness if the density contrast between lithosphere and asthenosphere is 100 kg/m^3 and that the Bouguer correction term

$$\Delta g_{RGA} = 2\pi k^2 \Delta\rho_{L/A} \Delta H_L$$

is applied, where Δg_{RGA}, $\Delta\rho_{L/A}$, ΔH_L are RGA difference, lithosphere/asthenosphere density contrast and lithospheric thickness difference, respectively.

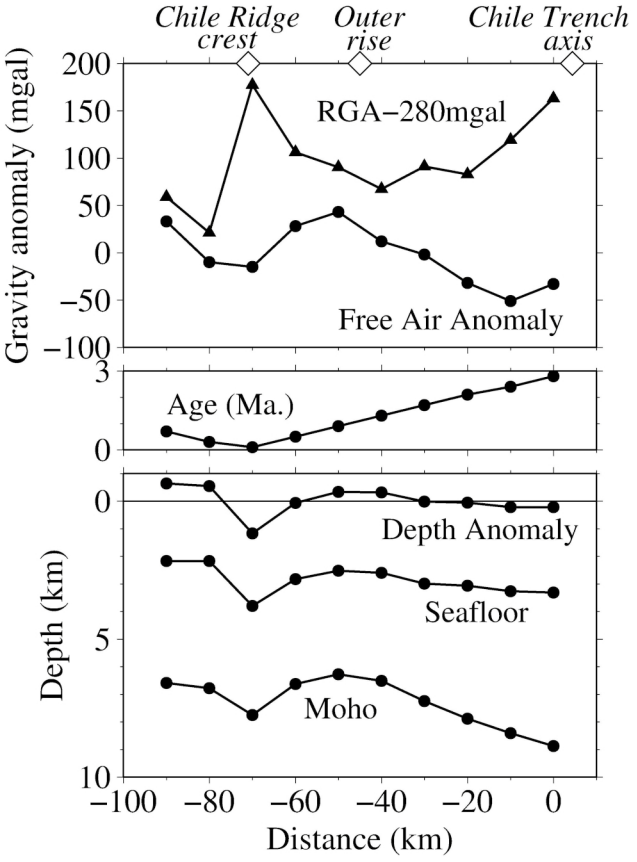

Fig. 8. Simplified geophysical profiles on the seaward side of the Chile Trench along Corridor 4 in Scherwath et al. (2009). The abscissa is the position on Corridor 4 in km from the trench axis (positive eastwards). Bottom: Depth of seafloor, Moho surface, both from the crustal P-wave velocity model in Fig. 3 in Scherwath et al. (2009), and depth anomaly based on the seafloor depth profile and the Crosby (2007) thermal model. Middle: Seafloor age along the profile based on Müller et al. (2008). Top: Free air anomaly along the Corridor 4 in figure 14 in Scherwath et al. (2009), and RGA (Residual Gravity Anomaly) calculated by use of the free air anomaly and crustal structure. See the text for details of how to calculate these geophysical parameters.

RGA as the proxy of the thickness of the subducting young lithosphere near both the Chile Ridge crest and the Chile trench axis was examined using the seismic and gravity data along the profile "Corridor-4" from Scherwath *et al*. (2009), an about 100 km-long profile that extends from the western flank of the ridge segment north of the CTJ to the trench axis (dashed line in Fig. 3). Figure 8 shows the result. The depth of the seafloor and Moho, and the free air anomaly are from Figs. 3 and 14 in Scherwath *et al*. (2009), respectively. Detailed layering within the crust was taken into account to calculate the RGA but is omitted in this figure. Age is derived from

Müller *et al*. (2008). Depth anomaly is calculated by subtracting the water depth by that predicted from the thermal model by Crosby (2007).

The result shows a relatively negative RGA on the Outer Rise and its rapid increase towards the trench axis. Together with other geophysical data, this suggests an elastic bending of the whole lithosphere and the consequent upwelling of the asthenosphere beneath the Outer Rise followed by a rapid lithospheric thickening towards the trench, even though the age of the oceanic crust is less than 3 Ma at this location. The depth anomaly shows an inverse pattern: shallower at the Outer Rise and deeper towards the trench. This implies heating of the oceanic crust in the outer rise and its cooling towards the trench axis. Rapid cooling of the old lithosphere towards the trench in the western Pacific has already been suggested by Tomoda and Fujimoto (1981) based on the RGA study. We suggest that similar rapid cooling takes place even in a very young (younger than 3 Ma) oceanic lithosphere. Note that the RGA maximum at the ridge crest (distance is –70 km) is due to a topographic deep at the median valley: a large amount of gravity correction was involved by replacing low-density water by high-density uppermost mantle. This is not a result of a thermal process but due to a tectonic stretching at the ridge crest.

Since the lithospheric thickness is proportional to the square root of its age, the rate of lithospheric thickening (dL/dt, where L is lithospheric thickness and t is lithospheric age) is inversely proportional to lithospheric thickness. Therefore, the lithosphere thickens rapidly under the ridge crest with a very thin initial lithosphere thickness as magmatic activity declines (as suggested by Figs. 5 and 7), maintaining the topographic features of the axial valley of the spreading ridge crest (Fig. 4(c)). This is also consistent with the results of the gravity study. Once the subduction started at the Chile Trench and the lithosphere under the ridge crest was amalgamated with the surrounding oceanic lithosphere, subduction may continue despite resistance from the relief of the former spreading ridge against the trench by the preceding "slab-pull" force driven by rapid lithospheric thickening underneath the trench, even after the "ridge-push" force disappears due to cessation of magma accretion at the ridge axis.

The profile of south of the CTJ (Fig. 6(d)) shows a very slight topographic high on the Antarctic Plate side. However, the positive free air anomaly, which is to be identified as the "Outer Gravity High," is clearly observed on the seaward side of the trench in this area. Even though the polarity of the age of the oceanic crust is opposite between Stage-1 (Fig. 6(a)) and Stage-4 (Fig. 6(d)), both elastic bending of the oceanic plate before subduction and abrupt lithospheric thickening near the trench axis may take place in both stages, which is the driving force behind the continuous subduction of the oceanic plate even after the spreading ridge subduction.

Acknowledgments—The authors would like to thank the onboard scientific party of the SORA2009 cruise for fruitful discussions. The authors also thank the crewmembers of R/V Mirai and JAMSTEC and GODI personnel who were engaged in the planning and operation of the cruise. A fruitful discussion with anonymous referees during the editing process is also to be acknowledged.

REFERENCES

Abe, N. (2009) Preliminary report on MR08-06 Leg1 Marine Geological and Geophysical Research: A complete trans-Pacific Cruise. *Eos Trans. AGU* **90**(52), Fall Meet. Suppl., abstract OS13A-1191.

Anma, R., Armstrong, R., Danhova, T., Orihashi, Y. and Iwane, H. (2006) Zircon sensitive high-mass-resolution ion microprobe U–Pb and fission-track ages for gabbros and sheeted dykes of the Taitao ophiolite, Southern Chile, and their tectonic implications. *Isl. Arc* **15**, 130–142.

Crosby, A. G. (2007) Aspects of the relationship between depth and age on the Earth and Moon. Ph.D. thesis, Univ. of Cambridge, Cambridge, U.K., 220 pp.

DeMets, C., Gordon, R. G., Argus, D. F. and Stein, S. (1994) Effect of recent revisions to the geomagnetic reversal time scale on estimates of current plate motions. *Geophys. Res. Lett.* **21**, 2191–2194.

D'Orazio, M., Agostini, S., Mazzarini, F., Innocenti, F., Manetti, P., Haller, M. J. and Lahsen, A. (2000) The Pali Aike Volcanic Field, Patagonia: slab-window magmatism near the tip of South America. *Tectonophysics* **321**, 407–427.

Hill, M. N. (1959) A median valley of the Mid-Atlantic Ridge. *Deep-Sea Res.* **6**, 193–205.

Isezaki, N. (1986) A new shipboard three-component magnetometer. *Geophysics* **51**(10), 1992–1998.

Lagabrielle, Y., Guivel, C., Maury, R. C., Bourgois, J., Fourcade, S. and Martin, H. (2000) Magnetic-tectonic effects of high thermal regime at the site of active ridge subduction: the Chile Triple Junction model. *Tectonophysics* **326**, 255–268.

Macdonald, K. C., Fox, P. I., Perram, L. J., Eisen, M. F., Haymon, R. M., Miller, S. P., Carbotte, S. M., Cormier, M.-H. and Shor, A. N. (1988) A new view of the mid-ocean ridge from the behaviour of ridge axis discontinuities. *Nature* **335**, 217–225.

Müller, R. D., Sdrolias, M., Gaina, C. and Roest, W. R. (2008) Age, spreading rates, and spreading asymmetry of the world's ocean crust. *Geochem. Geophys. Geosys.* **9**, Q04006, doi:10.1029.

Nafe, J. E. and Drake, C. L. (1957) Variation with depth in shallow and deep water marine sediments of porosity, density and the velocity of compressional and shear waves. *Geophysics* **22**, 523–552.

Scherwath, M., Contreras-Reyes, E., Flueh, E. R., Grevemeyer, I., Krabbenhoeft, A., Papenberg, C., Petersen, C. J. and Weinrebe, R. W. (2009) Deep lithospheric structures along the southern central Chile margin from wide-angle P-wave

modelling. *Geophys. J. Int.* **179**, 579–600.
Smith, A. D. (2003) A re-appraisal of stress field and convective roll models for the origin and distribution of Cretaceous to Recent intraplate volcanism in the Pacific basin. *Int. Geol. Rev.* **45**, 287–302.
Stern, C. R. (2004) Active Andean volcanism: its geologic and tectonic setting. *Rev. Geol. Chile* **31**, 161–206.
Tebbens, S., Cande, S., Kovacs, L., Parra, J., LaBrecque, J. and Vergara, H. (1997) The Chile ridge: A tectonic framework. *J. Geophys. Res.* **102**(B6), doi:10.1029/96JB02581.
Tilmann, F. J., Grevemeyer, I., Flueh, E. R., Dahm, T. and Goßler, J. (2008) Seismicity in the outer rise offshore southern Chile: Indication of fluid effects in crust and mantle. *Earth Planet. Sci. Lett.* **269**, 41–55.
Tomoda, Y. and Fujimoto, H. (1981) Gravity anomalies in the Western Pacific and geophysical interpretation of their origin. *J. Phys. Earth* **29**, 387–419.
Tomoda, Y., Fujimoto, H. and Matsumoto, T. (1983) Thickness difference of the lithosphere at the fracture zone and horizontal driving force of the plate. *J. Phys. Earth* **31**, 173–181.
Veloso, E. E., Anma, R. and Yamaji, A. (2009) Ophiolite emplacement and the effects of the subduction of the active Chile Ridge system: Heterogeneous paleostress regimes recorded in the Taitao Ophiolite (Southern Chile). *Andean Geol.* **36**(1), 3–16.
Watts, A. B. and Talwani, M. (1974) Gravity anomalies seaward of deep-sea trenches and their tectonic implications. *Geophys. J. R. astr. Soc.* **36**, 57–90.
Yoshii, T. (1972) Terrestrial heat flow and features of the upper mantle beneath the Pacific and the Sea of Japan. *J. Phys. Earth* **20**, 271–285.
Yoshii, T. (1973) Upper mantle structure beneath the North Pacific and the marginal seas. *J. Phys. Earth* **21**, 313–328.